ΣΥΝΕΔΡΙΑ ΤΗΣ 29ΗΣ ΜΑ·Ι·ΟΥ 1997

ΠΡΟΕΔΡΙΑ ΝΙΚΟΛΑΟΥ ΜΑΤΣΑΝΙΩΤΗ

ΦΥΣΙΚΗ. — **Transmission Mechanism of Seismic Electric Signals II,** by *P. Varotsos, N. Sarlis, M. Lazaridou* and *P. Kapiris**, διὰ τοῦ 'Ακαδημαϊκοῦ κ. Καίσαρος 'Αλεξοπούλου.

ABSTRACT

The present paper is a continuation of the paper published by *P. Varotsos et al.* (Practica of Athens Academy, **71**, 283-354, 1996) and investigates the frequency dependence of the electric field generated from a current electric dipole lying inside (or very close to) a highly conductive cylinder, of infinite length, embedded in a more resistive medium. The study is also extended to the case when the dipole is located inside (or very close to) a highly conductive layer, of infinite extent, embedded in a more resistive medium. The present considerations explain that preseismic electric signals (with frequency lower than 0.1 Hz can be detected at distances of the order of 100 km, in contrast to the coseismic ones (f〉〉0.1) Hz) that are strongly attenuated. Also the prominent role of the «edge effects» in the selectivity phenomenon of Seismic Signals is further discussed.

I. INTRODUCTION

The observation of very low frequency transient electric signals, less than 0.1 Hz (i.e., the so-called Seismic Electric Signals, SES) that are measured prior to earthquakes (EQ), revealed the so called *selectivity effect* (e.g., *Varotsos and Lazaridou* [1991]; *Varotsos et al.* [1993]); this effect consists of two facts (see also *Uyeda* [1996]): (i) SESs are observed at particular sites of the earth's surface («sensitive sites») and (ii) each «sensitive site» can collect

† In memory of Prof. *G. C. Vlachos*, former President of the Athens Academy.

* Π. ΒΑΡΩΤΣΟΥ, Ν. ΣΑΡΛΗ, Μ. ΛΑΖΑΡΙΔΟΥ καὶ Π. ΚΑΠΙΡΗ, **Ἕνα πιθανὸ πρότυπο γιὰ τὴν ἐξήγηση τῆς ἐπιλεκτικότητας τῶν Σεισμικῶν Ἠλεκτρικῶν Σημάτων (SES) II.**

SESs from certain focal areas, thus leading to a «*selectivity map*» for each measuring station. *Varotsos et al.* [1996; 1997 a, b] found that the selectivity effect is a direct consequence of Maxwell equations, if we consider that the EQ preparation zone lies in the vicinity of a conductive path for the transmission of the electric signal (e.g., recall that the resistivity ρ_f of a fault is 1-10 Ωm, while the resistivity of the host material is $\rho_0 = 10^3 - 10^4$ Ωm). By solving Maxwell equations, either numerically (*Varotsos et al.* [1996, 1997 b]) or analytically (*Varotsos et al.* [1997a]), we find that the electric field values exceed those of the artificial noise in two regions of the earth's surface: (i) around the top end of the conductive channel, as suggested in Fig. 25 of *Varotsos et al.* [1993] and (ii) just above the source (for usual EQ depths of 5-10 km). These solutions have been obtained in the static case. It is the object of the present paper to explain that similar conclusions can be achieved for frequencies smaller than 0.1 Hz. On the other hand, appreciably higher frequencies do not lead to detectable electric field values at epicentral distances of the order of 100 km or so. As we shall see in Ch. IV, the latter conclusion also explains that coseismic electric signals cannot be detected, in contrast to the SES.

II. CONDUCTIVE CYLINDER INSIDE A MEDIUM WITH SMALLER CONDUCTIVITY

A. Dipole current source at the center of the cylinder

We shall treat below only the low frequency (LF) case. Consider a conductive cylinder, of conductivity σ, with radius R and its axis along the z-axis, that lies in the region $\rho < R$. The remaining space is a medium with smaller conductivity σ', i.e., $\sigma' < \sigma$. Further, let us suppose that an electric emitting dipole $\mathbf{p} = \mathbf{I}l$ is located at the origin (0,0,0) of a cylindrical system (ρ,φ,z) of coordinates. A dipole $\mathbf{I}l = (0,0,Il)$, along the z-axis, will trigger the propagation of a Transverse Magnetic mode (TM_z) along the z-axis. We shall work in the Lorentz gauge; for this mode only the z-component A_z of the vector potential **A** is necessary for the description of the measured fields **E** and **H**. The fields **E** and **H** are expressed in terms of A_z, as follows:

$$E_\rho = (1/\sigma)\partial^2 A_z / \partial\rho\partial z,$$

$$E_\theta = (1/\sigma\rho)\partial^2 A_z / \partial\theta\partial z,$$

$$E_z = (1/\sigma)\,(\partial^2/\partial z^2 + k^2)A_z,$$

$$H_\rho = (1/\rho)\partial A_z/\partial\theta,$$

$$H_\theta = -\partial A_z/\partial\rho,$$

$$H_z = 0,$$

where $\omega = 2\pi f$ and $k^2 = i\mu\omega\sigma$, where μ is the magnetic permeability. In view of the axial symmetry, there is no θ-dependence of A_z, and hence the Helmholtz equation becomes

$$(1/\rho)\,\partial/\partial\rho(\rho\partial A_z/\partial\rho) + \partial^2 A_z/\partial z^2 + k^2 A_z = 0 \qquad (1)$$

The solutions of this equation can be separated as $\cos(\lambda z)J_0[\rho\sqrt{(k^2-\lambda^2)}]$ for the region inside the cylinder, and $\cos(\lambda z)H^{(1)}{}_0[\rho\sqrt{(k^2-\lambda^2)}]$ for the region outside the cylinder. $J_0(x)$ and $H^{(1)}{}_0(x)$are the Bessel and Hankel functions of the first kind (*Abramowitz and Stegun* [1972]) respectively, λ is a separation constant, and the square root should be taken as $\sqrt{z} = |z|^{1/2}e^{iArg(z)/2}$, where Arg(z) is measured anticlockwise from the real axis.

To the solution of the homogeneous Eq.(1), one has to add the primary (singular) $A_{zprimary}$ field due to a unit electric dipole (*Gradhsteyn and Ryzhik* [1980], see Eq. 6.677.8, p. 737)

$$A_{zprimary} = e^{ikr}/(4\pi r) = (i/4\pi)\int_0^\infty \cos(\lambda z)H^{(1)}{}_0[\rho\sqrt{(k^2-\lambda^2)}]d\lambda, \qquad (2)$$

where $r = (\rho^2 + z^2)^{1/2}$, and satisfy the boundary conditions

$$\sigma E_{\rho IN} = \sigma' E_{\rho OUT},\ E_{zIN} = E_{zOUT},\ \text{and}\ H_{\theta IN} = H_{\theta OUT}$$

at $\rho = R$. We finally obtain:

$$A_{zIN} = A_{zprimaty} + \int_0^\infty A(x)\cos(xz/R)J_0[(\rho/R)\sqrt{(k^2R^2 - x^2)}]dx, \qquad (3)$$

$$A_{zOUT} = \int_0^\infty B(x)\cos(xz/R)H^{(1)}{}_0[(\rho/R)\sqrt{(k'^2R^2 - x^2)}]dx, \qquad (4)$$

where A(x) and B(x) are determined from the two relations:

$$A(x) = [n'B(x)H'^{(1)}_0(n') - n(i/4\pi R)H'^{(1)}_0(n)]/[nJ'_0(n)],$$

$$B(x) = (n/n')^2(\sigma'/\sigma)\,(1/8\pi^2 Rn)/[J_0'(n)H^{(1)}_0(n') - (\sigma'/\sigma)(n/n')J_0(n)H'^{(1)}_0(n')],$$

where $n = \sqrt{(k^2R^2 - x)}$ and $n' = \sqrt{(k'^2R^2 - x^2)}$, $k'^2 = i\mu\omega\sigma'$.

It is easily verified (Gradshteyn and Ryznik [1980], see Eq. 8.406 and 8.407, p. 952) that in the limit $f \to 0$, the solution of Eqs. (3) and (4) results to the solution of the static case given by *Varotsos et al.* [1997a].

In the limit of long distances, i.e., $z/R \to \infty$, the main contribution in the integral of Eq. (4) comes from B(0), which tends to*

$$(i/4\pi R)\{n(0)H'^{(1)}_0[n(0)])\}/\{n'(0)H'^{(1)}_0[n'(0)]\}, \tag{5}$$

and hence the electric field, resulted from Eq. (5), is given by:

$$E_{zOUT} = (1/\sigma')(\partial^2/\partial z^2 + k'^2)A_z = \int_0^\infty (k'^2R^2 - x^2)B(x)\cos(xz/R)\,H^{(1)}_0[(\rho/R)\sqrt{(k'^2R^2 - x^2)}]/(\sigma' R^2)dx. \tag{6}$$

Now we discriminate two cases as far as the frequency range is concerned: For appreciably low frequencies so that k^2R^2 and $k'^2R^2 \to 0$, only the contribution from $x \to 0$ is significant and $B(x \to 0) \to i/4\pi R$; the integral of Eq. (6) then results in the expression for the electric field in a full space of conductivity σ' (i.e. see Eq. 2) and hence its attenuation is governed by a «skin depth» δ_{OUT} corresponding to the outer medium. For higher frequencies, (i.e., $f > f_c$ for the definition of f_c see below), the electric field is attenuated with a «skin depth» significantly smaller than that for a full space of conductivity σ' having, of course, as a lower limit the «skin depth» δ_{IN} corresponding to a full space of conductivity σ (*Sommerfeld* [1967]; *Goubeau* [1967]).

A detailed study of the electric field E_{zIN} inside the cylinder can be done with the help of the expression:

$$E_{zIN} = [i/(4\pi\sigma R^3)]\int_0^\infty (k^2R^2 - x^2)\Gamma(x)\cos(xz/R)dx, \tag{7}$$

---

* By substituting the Wronski determinant in the expansion of B(x) and then taking the limit.

where

$$\Gamma(x) = H^{(1)}{}_0[(\rho/R)n] - J_0[(\rho/R)n]\{H'^{(1)}{}_0(n)H^{(1)}{}_0(n') - [n\sigma'/(n'\sigma)]H^{(1)}{}_0(n)H'^{(1)}{}_0(n')\}/$$
$$\{J'_0(n)H^{(1)}{}_0(n') - [\sigma' n/(\sigma n')]J_0(n)H'^{(1)}{}_0(n')\}.$$

For the case of our interest, i.e., $\sigma/\sigma' > 1$, we have the following limiting cases:

(a) At small distances, i.e., $r/R \to 0$, only the first term of $\Gamma(x)$ is singular. This leads to a behavior of the electric field governed by the inner medium and resembles either the static result if $R/\delta_{IN} < 1$, or the dynamic one (i.e. attenuation) if $R/\delta_{IN} > 1$.

(b) At long distances, i.e., $r/R \to \infty$, the contribution from $\Gamma(0)$ dominates the integral of Eq. (7). For appreciably low frequencies so that k^2R^2 and $k'^2R^2 \to 0$, the derivatives $H'^{(1)}{}_0(n)$ and $H'^{(1)}{}_0(n')$ dominate in $\Gamma(x)$, thus leading to $\Gamma(0) \to (n'/n)^2(\sigma/\sigma')H^{(1)}{}_0(n')$: this result, when considering Eqs. (2) and (7), indicates that the electric field is solely determined by the resistivity of the outer medium, as we discussed previously. On the other hand, for higher frequencies, (i.e., $f > f_c$ for the definition of f_c see below), the electric field is attenuated with a «skin depth» significantly smaller than that for a full space of conductivity σ' having, of course, as a lower limit the «skin depth» δ_{IN} corresponding to a full space of conductivity σ (*Sommerfeld* [1967]; *Goubeau* [1950]).

(c) At intermediate distances, three cases can be distinguished:

(c1) When $(d/R)_{crit}R > 5\delta_{OUT}$, where $(d/R)_{crit}$ was defined by *Varotsos et al.* [1997a], the attenuation of the electric field is determined as in case (b).

(c2) When $(d/R)_{crit}\,R < 5\delta_{OUT}$, and $n^2(0) < 1$, i.e. $f < f_c \equiv 1/(2\pi\mu\sigma R^2)$, all the approximations made in the discussion of the static result by *Varotsos et al.* [1997a] hold; we then observe all the main features of the static dependence up to a distance $\approx 5\delta_{OUT}$, while at longer distances, the attenuation is governed by the resistivity of the outer medium as in case (b). From physical point of view, this means that the distance d is appreciably smaller than the «wavelength» in the external medium, and the radius R appreciably smaller than the «wavelength» in the highly conductive medium (so that enough energy enters from the conductive path into the more resistive medium).

(c3) When $(d/R)_{crit}R < 5\delta_{OUT}$, and $n^2(0) > 1$, i.e. $f > f_c \equiv 1/(2\pi\mu\sigma R^2)$; these two inequalities are compatible when $(d/R)^2{}_{crit}(\sigma/\sigma') < 50$; Now if we also consider the results by *Varotsos et al.* [1997a], as far a the values of

$(d/R)_{crit}$ is concerned, this implies that (since $\sigma/\sigma' > 1$) it can only happen when $\sigma \approx \sigma'$; however, in such a case, no significant current channelling effects will be observed.

In Fig. 1, we plot the electric field E_{inside} inside the channel (on the axis

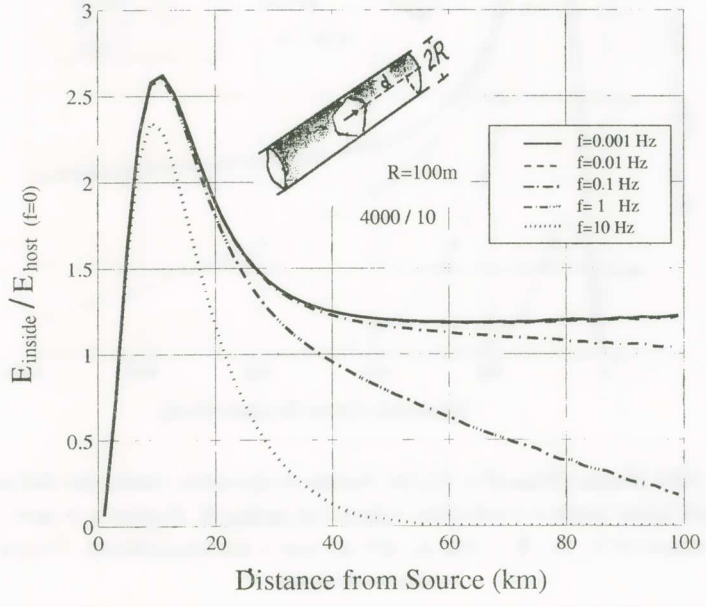

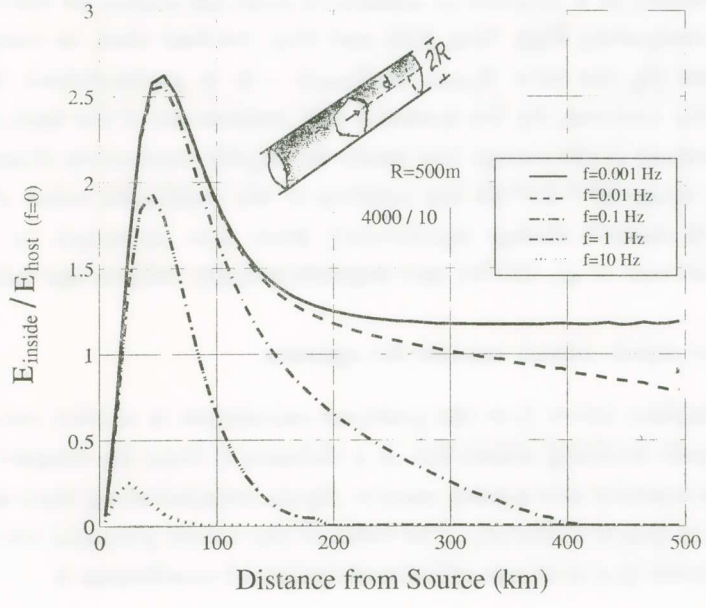

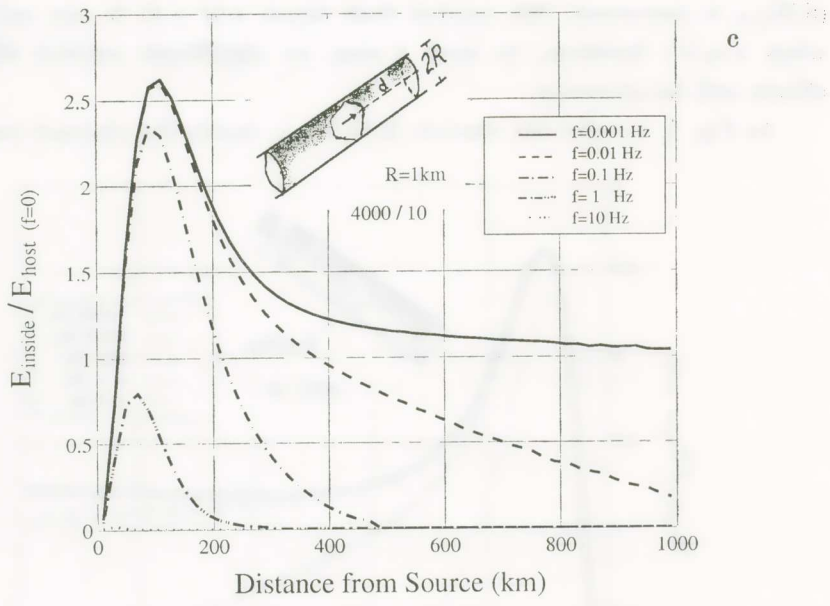

Fig. 1. The ratio $|E_{inside}| / |E_{host}(f = 0)|$, for various frequencies, versus the distance d from a current dipole lying inside a conductive cylinder of radius R. Figures a, b and c correspond to various values of R, i.e., R = 100 m, 500 m, and 1 km respectively. Conductivity ratio $\sigma/\sigma' = 4000/10$.

of the cylinder) as a function of distance d from the source for various values of R. By comparing Figs. 1(a), 1(b) and 1(c), we find that, as manifested in Eqs. (3) and (4), the ratio $E_{inside}(f)/E_{host}(f = 0)$ is parametrized, for a given conductivity contrast, by the quantity fR^2, reminecent of the term k^2R^2, that gives a measure of the energy loss inside the *highly* conductive channel. In the frequency range 10^{-3}–10^{-1}Hz the position of the maximum value of $E_{inside}(f)/E_{host}$ (f=0) doesn't change significantly from that estimated by the static result, (*Varotsos et al.*, 1997a), and depends roughly only on the value of d/R.

B. Current dipole source outside the cylinder

We explain below how the previous calculation is carried out when the (point) dipole emitting source lies at a distance D from the conductive cylinder. Let us consider now a point current dipole, oriented along the z-axis, which is located at $(\rho,\varphi,z) = (D,0,0,)$. The value of the vector potential for such a dipole at a point (ρ,φ,z) of our cylindrical system of coordinates is

$$A_{z\text{primary}} = \exp(ik'\mathcal{R}) / (4\pi\mathcal{R}) = (i/4\pi)\int_0^\infty \cos(\lambda z)H^{(1)}{}_0[\sqrt{[\rho^2+D^2-2\rho D\cos(\varphi)]}\sqrt{(k'^2-\lambda^2)}]\, d\lambda, \quad (8)$$

where $\mathcal{R} = \sqrt{[\rho^2 + D^2-2\rho D\cos(\varphi) + z^2]}$. Using Eq. 8.531.2 (*Gradshteyn and Ryzhik* [1980]), we can obtain the expansion of this vector potential into separated solutions of the Helmholtz equation in cylindrical coordinates for points of $\rho < D$ and $\rho > R$:

$$A_{z\text{primary}} = (i/4\pi)\Sigma_{n=0}^{\infty} \varepsilon_n \cos(n\varphi) \int_0^\infty \cos(xz/R) J_n[(\rho/R)\sqrt{(k'^2R^2-x^2)}]H^{(1)}{}_n[(D/R)\sqrt{(k'^2R^2-x^2)}]dx, \quad (9)$$

where $\varepsilon_n = 1$ for $n = 0$ and $\varepsilon_n = 2$ otherwise.

In order to find either the electric field on the axis of the cylinder or the total current inside the cylinder, we only need the radially symmetric $n = 0$ contribution of the above sum. Moreover, from elementary group theory we know that the sector $n = 0$ will not be mixed with the $n \neq 0$ sectors. Thus, for this sector we can write

$$A_{zIN(n=0)} = (i/4\pi)\int_0^\infty A_0(x)\cos(xz/R)J_0[(\rho/R)\sqrt{(k^2R^2-x^2)}]dx, \quad (10)$$

and

$$A_{zOUT(n=0)} = \int_0^\infty B_0(x)\cos(xz/R)H^{(1)}{}_0[(\rho/R)\sqrt{(k'^2R^2-x^2)}]dx + A_{z\text{primary}(n=0)}. \quad (11)$$

By considering that the boundary conditions

$$\sigma E_{\rho IN} = \sigma' E_{\rho OUT}, E_{zIN} = E_{zOUT}, \text{ and } H_{\theta IN} = H_{\theta OUT}$$

at $\rho = R$, have to be satisfied by the electromagnetic fields obtained from the $n = 0$ sector vector potentials of Eqs. (10) and (11), we finally obtain:

$$A_0(x) = (n'^2/n)H^{(1)}{}_0(n'D/R)[J_0(n')H'^{(1)}{}_0(n') - J'_0(n')H^{(1)}{}_0(n')]/ [n(\sigma'/\sigma)J_0(n)H'^{(1)}{}_0(n') - n'J'_0(n)H^{(1)}{}_0(n')] \quad (12)$$

The total E_z component at $\rho = 0$ will depend only on the $n = 0$ sector since for $n \neq 0$ the respective contribution will involve $J_n(\rho = 0)$ which for $n \neq 0$ equals zero.

At long distances from the source, $z/R \to \infty$, the contribution in the integral of Eq. (10) will come from $x = 0$. At this limit the most singular function of Eq.(12) is $H'^{(1)}_0(n')$, thus leading $A_0(x)$ to the value $A_0(x \to 0) \to [n'(0)/n(0)]^2 (\sigma/\sigma')H^{(1)}_0[n'(0)D/R]$. This result in view of Eq.(9), reveals that $E_z(\rho = 0)$ is that obtained for a full space of conductivity σ' due to a point current dipole at (D,0,0). Thus, the field at a point (0,0,z) far away from the source and inside the channel will not be significantly affected by the distance D since $D << z$, exactly as it happens for the static result (*Varotsos at al.* [1997a]).

III. CONDUCTIVE LAYER INSIDE A MEDIUM WITH SMALLER CONDUCTIVITY

A. Current dipole source inside the layer

The analytical solution can be found in terms of a two-dimensional Fourier transform of the Schelkunoff potentials (*Schelkunoff* [1937, 1943], *Stratton* [1941], *Ward and Hohmann* [1994]). Consider a conductive layer, with conductivity σ (and infinite extent) that is parallel to the xz plane of the cartesian system. We assume that this layer has a width w, e.g., the layer extends from $y = -w/2$ to $y = w/2$, the conductivity of the surrounding medium is σ'. Consider an electric current dipole source $\mathbf{Il}$ along the z-axis, i.e., parallel to the surfaces of the layer, located at the origin. This produces a xz-Fourier transformed vector potential (*Gradshteyn and Ryzhik*, Eqs. 8.511.4,6.616.12).

$$\begin{aligned} A_z(k_x,k_z,y) &= \int_{-\infty}^{\infty}\int_{-\infty}^{\infty}[Il\exp(ikr)/4\pi r]\exp[-i(k_x x+k_z z)]dxdz = \\ &= (Il/2)\exp(-u|y|)/u, \end{aligned} \tag{13}$$

where $u^2 = k_x^2+k_z^2-k^2$ and $k^2 = i\mu\sigma\omega$. The electromagnetic fields of such a vector potential can be decomposed to transverse magnetic (TM_y) and transverse electric (TE_y)y-modes.

Recalling that the definition for the real space Schelkunoff potential A_y is $\mathbf{A} = A_y\mathbf{e}_y$, $\mathbf{E} = (1/\sigma)\nabla \times \mathbf{B}$, $\mathbf{B} = \nabla \times \mathbf{A}$, the TM_y mode has an xz-Fourier transformed Schelkunoff potential A_y,

$$A_{y\text{primary}} = -(Il/2)ik_z[\exp(-u|y|)/(k_x^2+k_z^2)]\,\text{sign}(y), \tag{14}$$

where $\text{sign}(y) = y/|y|$. Furthermore, recalling the definition for the real space

Schelkunoff potential F_y is $\mathbf{F} = F_y\mathbf{e}_y$, $i\mu\omega\mathbf{B} = \nabla \times \mathbf{E}$, $\mathbf{E} = \nabla\times\mathbf{F}$, the TE_y mode has an xz-Fourier tranformed Schelkunoff potential F_y,

$$F_{y\text{primary}} = [\mu\omega Il/(2u)]k_x\exp(-u|y|)/(k_x^2+k_z^2), \tag{15}$$

The contributions of $A_{y\text{primary}}$ and $F_{y\text{primary}}$ in $\mathbf{E}$ and $\mathbf{B}$, when added give the correct electric dipole electromagnetic fields given by Eq. (13).

The following boundary conditions (see Ward and Hohmann [1994] pp. 150-158) have to be satisfied:

a) for the TM_y mode A_y and $(1/\sigma)\partial_y A_y$ continuous at $y = \pm\ w/2$, and

b) for the TE_y mode F_y and $\partial_y F_y$ continuous at $y \pm w/2$.

Using as primary potentials those of Eqs. (14) and (15), we obtain that the secondary potentials are:

a) for the TM_y mode

$$A_{y\text{secondary}} = -(Il/2)ik_z[\exp(-u'|y|)/(k_x^2+k_x^2)]\text{sign}(y)\exp(u'w/2)/ \{[(\sigma u')/(\sigma' u)]\sinh(uw/2)+\cosh(uw/2)\},\ \text{for}|y|\geq w/2 \tag{16}$$

and

$$A_{y\text{secondary}} = (Il/2)ik_z[\exp(-uw/2)/(k_x^2+k_z^2)]\sinh(uy)[(\sigma u')/(\sigma' u)-1]/ \{[(\sigma u')/(\sigma' u)]\sinh(uw/2)+\cosh(uw/2)\},\ \text{for}\ |y|<w/2 \tag{17}$$

b) for the TE_y mode

$$F_{y\text{secondary}} = [\mu\omega Il/(2u)]k_x[\exp(-u'|z|)/(k_x^2+k_z^2)]\exp(u'w/2)/ [(u'/u)\cosh(uw/2) + \sinh(uw/2)],\ \text{for}\ |y| \geq w/2 \tag{18}$$

and

$$F_{y\text{secondary}} = [\mu\omega Il/(2u)]k_x[\exp(-uw/2)/(k_x^2+k_z^2)]\ (1-u'/u) \cosh(uz)/[(u'/u)\cosh(uw/2)+\sinh(uw/2)],\ \text{for}\ |y|<w/2. \tag{19}$$

An inspection of Eqs. (16), (17), (18) and (19) leads to the following remarks:

a) At small distances from the source, i.e. $x^2 + z^2 \to 0$, the contribution in the Fourier transform comes from $u \to \infty$ and $u' \to \infty$; in such a case the terms

exp(-uw/2) in Eqs.(17) and (19) describe the rapid attenuation of the secondary potentials thus reflecting that, at small distances the fields are solely determined by the inner medium.

b) At large distances from the source and for small frequencies, i.e. below some

$$f_0 = 1/(\mu\sigma w^2), \tag{20}$$

we have, since the contribution comes from the $u \to \sqrt{(-k^2)}$ limit, $|\cosh(uw/2)| \to 1$ and $|\sinh(uw/2)| \to 0$. In such a case, the total field —which is determined by the secondary potentials of Eqs.(16-19)— follows practically the properties of the external more resistive medium. The attenuation for a full space of conductivity σ' has an asymptotic expression for the amplitude of the electric field at large distances of the form $\exp[-r/\delta_{OUT}(f)]/r^2$. (see Ward and Hohmann [1994], p. 173). For higher frequencies, (i.e. $f > f_0$), the electric field is attenuated with a «skin depth» significantly smaller than that for a full space of conductivity σ' having, of course, as a lower limit the «skin depth» δ_{IN} corresponding to a full space of conductivity σ.

c) In the intermediate region, where the main contribution in the Fourier transform is from intermediate $k_x^2 + k_z^2$ so that $[(\sigma u')/(\sigma' u)]\sinh(uw/2) + \cosh(uw/2) \approx \sigma u' w/(2\sigma') + 1$ and $\sigma u' w/(2\sigma') >> 1$, a dependence $E \propto 1/r^2$ results.

Note that the transition from the limiting case (c) to the limiting case (b) is continuous. Therefore, we could accept, for small frequencies, an approximate expression of the form $\exp[-r/\delta_{OUT}(f)]/r^2$, for intermediate-long distances. In order to verify the validity of this approximation, we proceed to the following example: In Fig. 2 we plot, in the frequency range $10^{-3} - 10$Hz, the electric field E_z, measured at points on the z-axis, versus the distance d from the dipole (with parameter the width of the layer), we observe that, as explained, the static approximation is valid as long as the distance from the dipole is small compared to the wavelength in the host medium. Furthermore, we notice that there is a certain distance at which the ratio $E_{inside}(f)/E_{host}(f=0)$ acquires a maximum value; according to the above discussion, the position of this maximum can be approximately determined by the expression:

$$E_{inside}(f)/E_{host}(f=0) \propto r \exp[-r/\delta_{OUT}(f)].$$

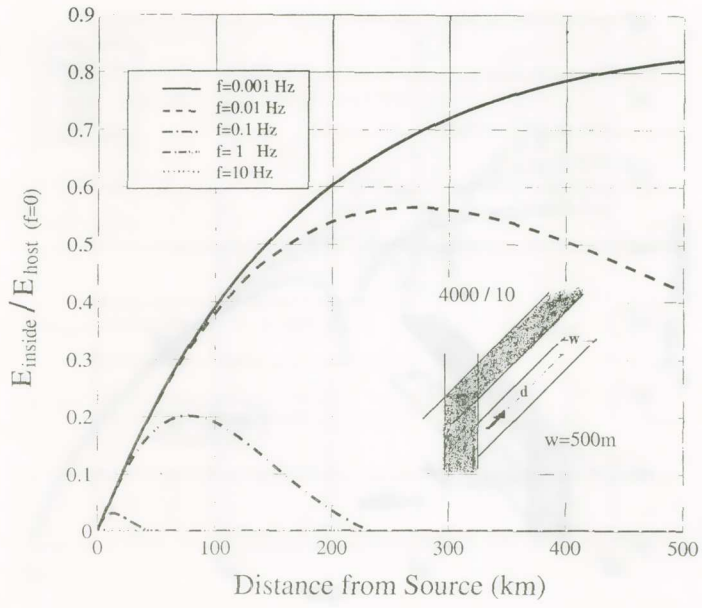

Fig. 2. The ratio $|E_{inside}|/|E_{host}|$ versus the reduced distance d/w from a current dipole lying inside a conductive layer of infinite extent (width w, conductivity σ'). Conductivity ratio $\sigma/\sigma' = 4000/10$. The curves corrrspond (see the inset) to various frequencies, i.e., 10^{-3}, 10^{-2}. 10^{-1}, 1 and 10 Hz.

An inspection of the curves of Fig. 2, which have been obtained from the full analytical expression, leads to the conclusion that the position of the maximum, in each curve, is in fair agreement with $r_{max} = \delta_{OUT}(f)$, which results from the aforementioned approximation.

B. Current dipole outside the layer

When the z-electric dipole lies at a distance h (cf. h = D–w/2, see Figs. 3 and 4) from its closest surface of the conductive layer (we draw attention that this layer is now located between the plane y = 0 and y = w), the following boundary conditions should hold

a) for the TM_y mode A_y and $(1/\sigma)\partial_y A_y$ continuous at y = 0 and y = w, and

b) for the TE_y mode F_y and $\partial_y F_y$ continuous at y = 0 and y = w,

we can obtain the following results for the Schelkunoff potentials inside the conductive layer, i.e. $y \in [0,w]$:

a) For the TM_y mode:

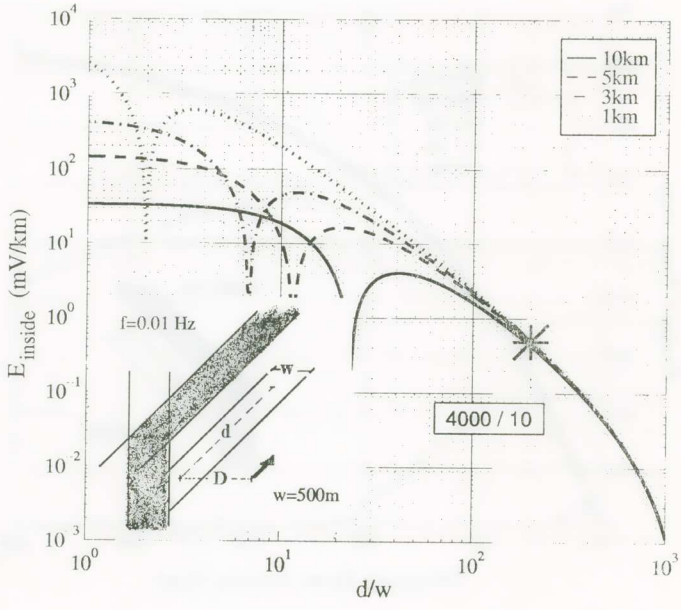
a
10km
5km
3km
1km
f=0.01 Hz
w
d
D
w=500m
4000 / 10
E inside (mV/km)
d/w

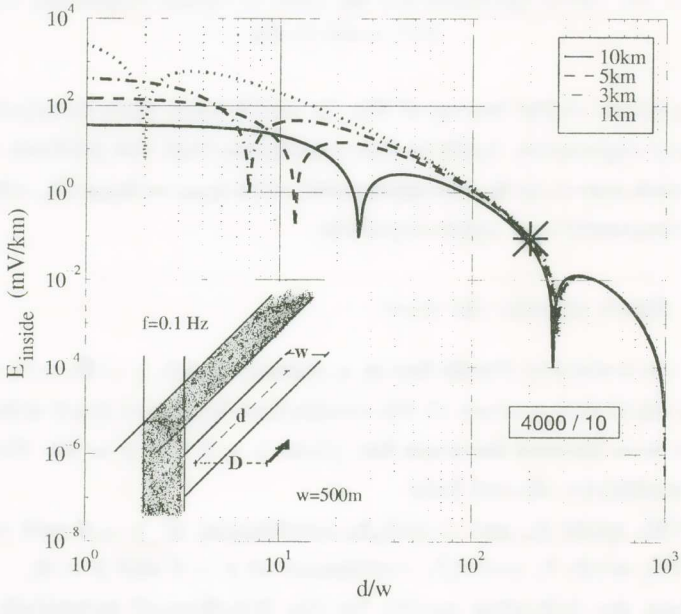
b
10km
5km
3km
1km
f=0.1 Hz
w
d
D
w=500m
4000 / 10
E inside (mV/km)
d/w

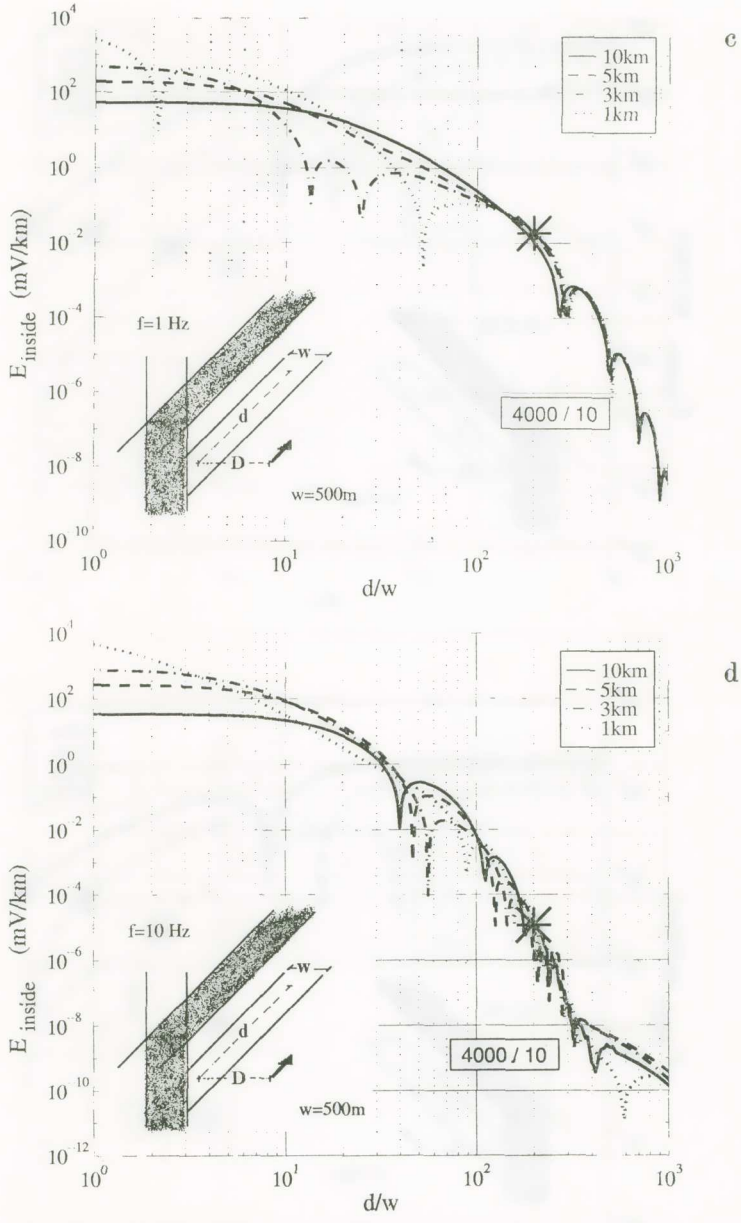

Fig. 3. The absolute values of E_{inside} versus d/w, for various values of the distance D (= 1, 3, 5, 10 km, see the inset) of the emitting dipole from a given conductive layer (w = 500 m). Note that, for values d/w = 10^2 or larger, all curves practically coincide. Conductivity ratio σ/σ'=4000/10. Figures a, b, c and d correspond to various frequencies, i.e., 0.01 Hz (a), 0.1 Hz (b), 1 Hz (c) and 10 Hz (d). The source was taken 2.26×10^3 A. km for reasons discussed by *Varotsos et al.* [1997a], i.e., it might correspond to an earthquake with magnitude 5.0.

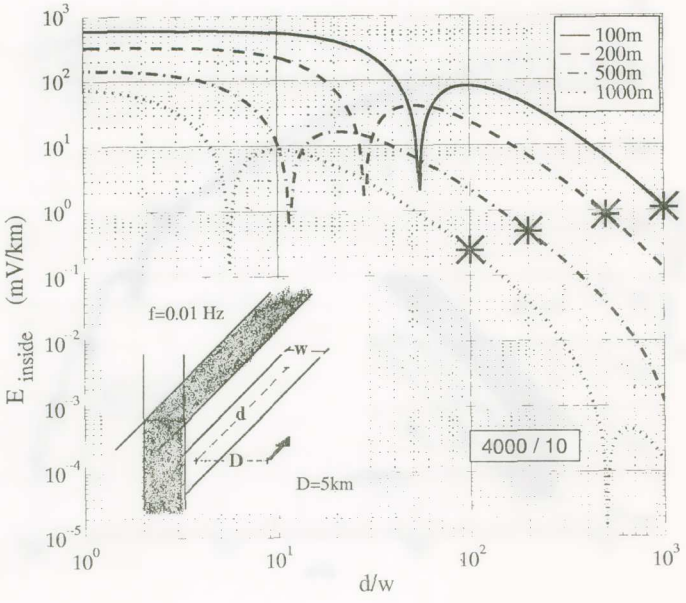
100m
200m
500m
1000m
f=0.01 Hz
w
d
D
D=5km
4000 / 10
E inside (mV/km)
d/w

a

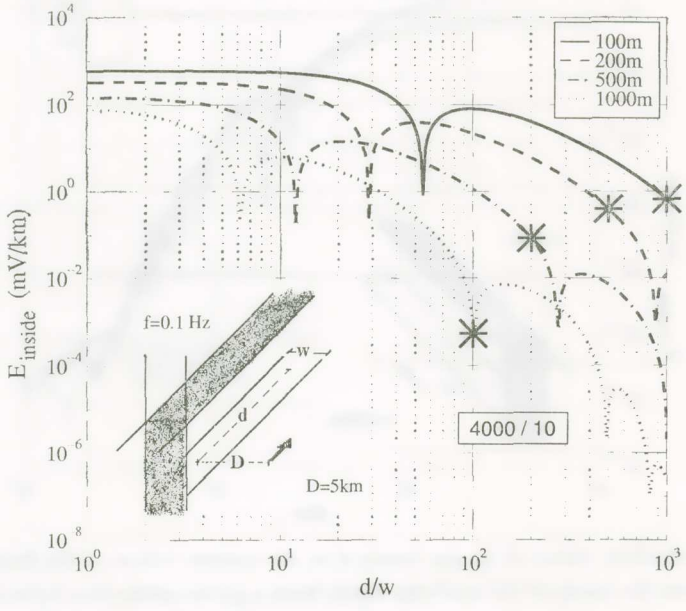
100m
200m
500m
1000m
f=0.1 Hz
w
d
D
D=5km
4000 / 10
E inside (mV/km)
d/w

b

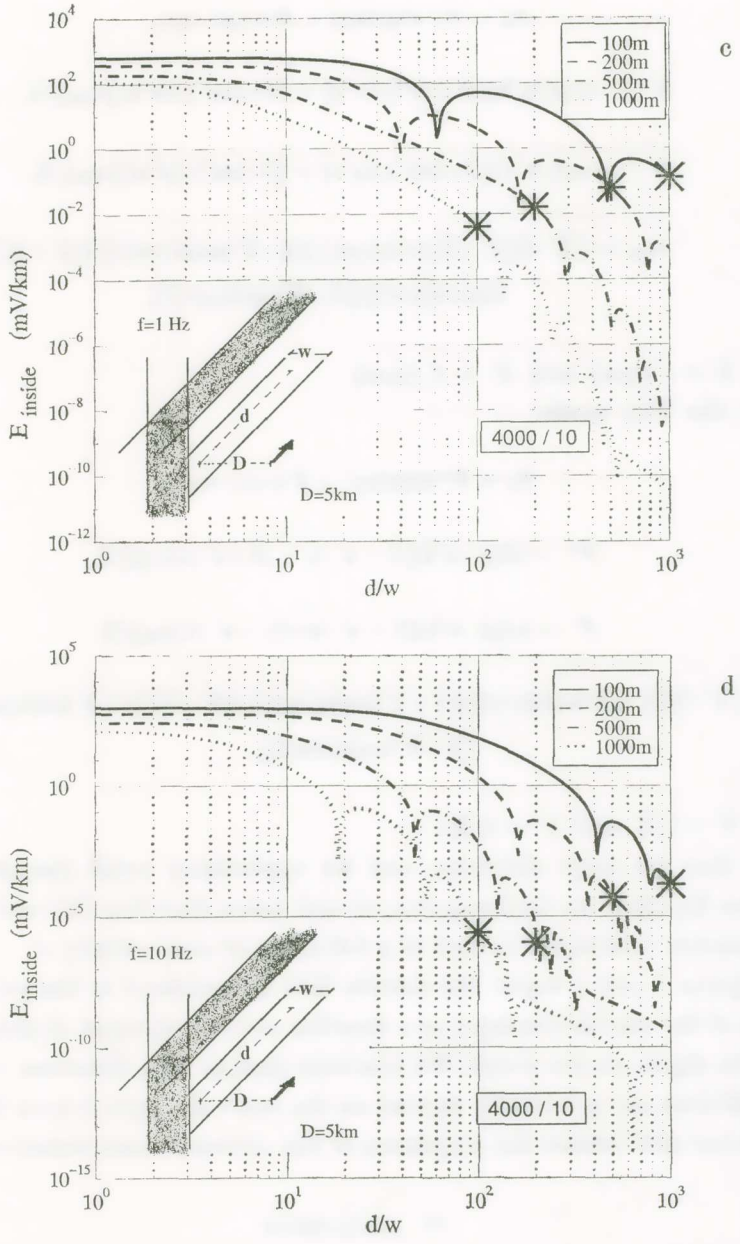

Fig. 4. The absolute values of E_{inside} versus d/w, for various values of the width w (= 100, 200, 500, 1000 m, see the inset) of a conductive layer, but for the same D-value, i.e., D=5 km. The points with asterisks correspond to d=100 km. Conductivity ratio σ/σ'=4000/10. Figures a, b, c and d correspond to various frequencies, i.e., f = 0.01, 0.1, 1 and 10 Hz respectively. The source was taken 2.26×10^3 A. km for reasons discussed by *Varotsos et al.* [1997a].

$$A_y = A^+\exp(uy) + A^-\exp(-uy), \tag{21}$$

$$A^+ = \exp(-u'h)\{1-(\sigma u')/(\sigma' u) + [1+(\sigma u')/(\sigma' u)]r_{TM}\}/2, \tag{22}$$

$$A^- = \exp(-u'h)\{1+(\sigma u')/(\sigma' u) + [1-(\sigma u')/(\sigma' u)]r_{TM}\}/2, \tag{23}$$

$$r_{TM} = \{Z'-Z[Z'+Z\tanh(uw)]/[Z+Z'\tanh(uw)]\}/\{Z'+Z[Z'+Z\tanh(uw)]/[Z+Z'\tanh(uw)]\}, \tag{24}$$

where $Z = \sigma/(i\mu\omega)$ and $Z' = \sigma'/(i\mu\omega)$.

b) For the TM_y mode:

$$F_y = F^+\exp(uy) + F^-\exp(-uy), \tag{25}$$

$$F^+ = \exp(-u'h)[1 - u'/u + (1+u'/u)r_{TE}]/2, \tag{26}$$

$$F^- = \exp(-u'h)[1 + u'/u+(1 - u'/u)r_{TE}]/2, \tag{27}$$

$$r_{TE} = \{Y'-Y[Y'+Y\tanh(uw)]/[Y+Y'\tanh(uw)]\}/\{Y'+Y[Y'+Y\tanh(uw)]/[Y+Y'\tanh(uw)]\}, \tag{28}$$

where $Y = 1/Z$ and $Y' = 1/Z'$.

Notice that for large distances, and for appreciably small frequencies (i.e., $f<f_0$, see Eq.(20)), we find $r_{TM}=r_{TE}=0$ and hence that Eqs.(21) and (25) lead to an electric field equal to that of a full space of conductivity σ'.

Figures 3 and 4 depict the electric field E_z measured at the points in the middle of the conductive layer as a function of the projection of their distance from the dipole on the z-axis. We conclude that, at long distances, i.e. $d>>D$, the field does not practically depend on the exact distance D from the conductive layer and follows the properties of the external more resistive medium.

IV. DISCUSSION

We mainly focus our discussion below on two points: (i) how the absence of a coseismic electric signal is explained on the basis of the considerations of the present paper and (ii) why earlier calculations by other authors failed to explain the selectivity effect.

a. On the absence of a coseismic electric signal from the VAN records

Laboratory measurements of the electric signals emitted from solids under gradually increasing stress were the subject of various publications. *Yoshida et al.* [1997] confirm the findings of similar experiments by our group (*Hadjicontis and Mavromatou* [1994, 1995, 1996]; *Mavromatou* [1995]; and *Mavromatou and Hadjicontis* [1994]). *Yoshida et al.* [1997] studied granite blocks only, while Hadjicontis and coworkers extended the measurements to various types of rock samples. Both groups observed «preseismic» and «coseismic» electric changes and also find that the «coseismic» signal has an amplitude appreciably larger than that of the «preseismic». Furthermore, *Yoshida et al.* [1997] confirm the earlier finding of our group that, for low stress changes (i.e., for which the time scale is larger than the relaxation time $\tau = \varepsilon/\sigma$, where ε denotes the permitivity and σ the conductivity), «the [preseismic] electric signal... is proprtional to the time derivative of the stress change». *Yoshida et al.* [1997] also reported that «Even if we measure the high-frequency components, the preseismic signal does not have high-frequency components. In contrast, higher-frequency components appear with higher amplitude at the onset of the coseismic signal». «... The preseismic signal did not contain high-frequency components». These observations were also reported by *Hadjicontis and Mavromatou* [1995, 1996] and, as it will be explained below, seem to have a decisive importance for the explanation of the non-detectability of significant coseismic changes in SES measurements at large epicentral distances.

The effective «wavelength» λ_{ef} (and hence the corresponding «skin depth» $\delta_{ef} \approx \lambda_{ef}/6.28$) for the transmission of a signal (of frequency f) emitted from a current dipole lying in the vicinity of a conductive path, with conductivity σ', embedded in a more resistive medium was studied above. It was found that, for low frequencies [i.e., $f < f_c$; for example, for a cylindrical path of radius R, the frequency f_c is determined from the condition $R^2(\mu 2\pi f_c/\rho_f) << 1$, as mentioned above], λ_{ef} is approximately equal with the «wavelength» λ, which corresponds to a full volume with conductivity σ; for higher frequencies (i.e., $f > f_c$), the value of λ_{ef} is significantly smaller than λ. Since $\lambda^2 = 10^7/(f\sigma)$ (where σ is in $\Omega^{-1}m^{-1}$ and f in Hz), we find that $\lambda_{ef} \approx \lambda = 632$ km (and hence $\delta \approx 100$ km), if $f \approx 0.1$ Hz and $\rho \approx 4 \times 10^3 \Omega m$. In order words, signals with frequencies appreciably larger than 0.1 Hz (and hence the coseismic electric signals) are

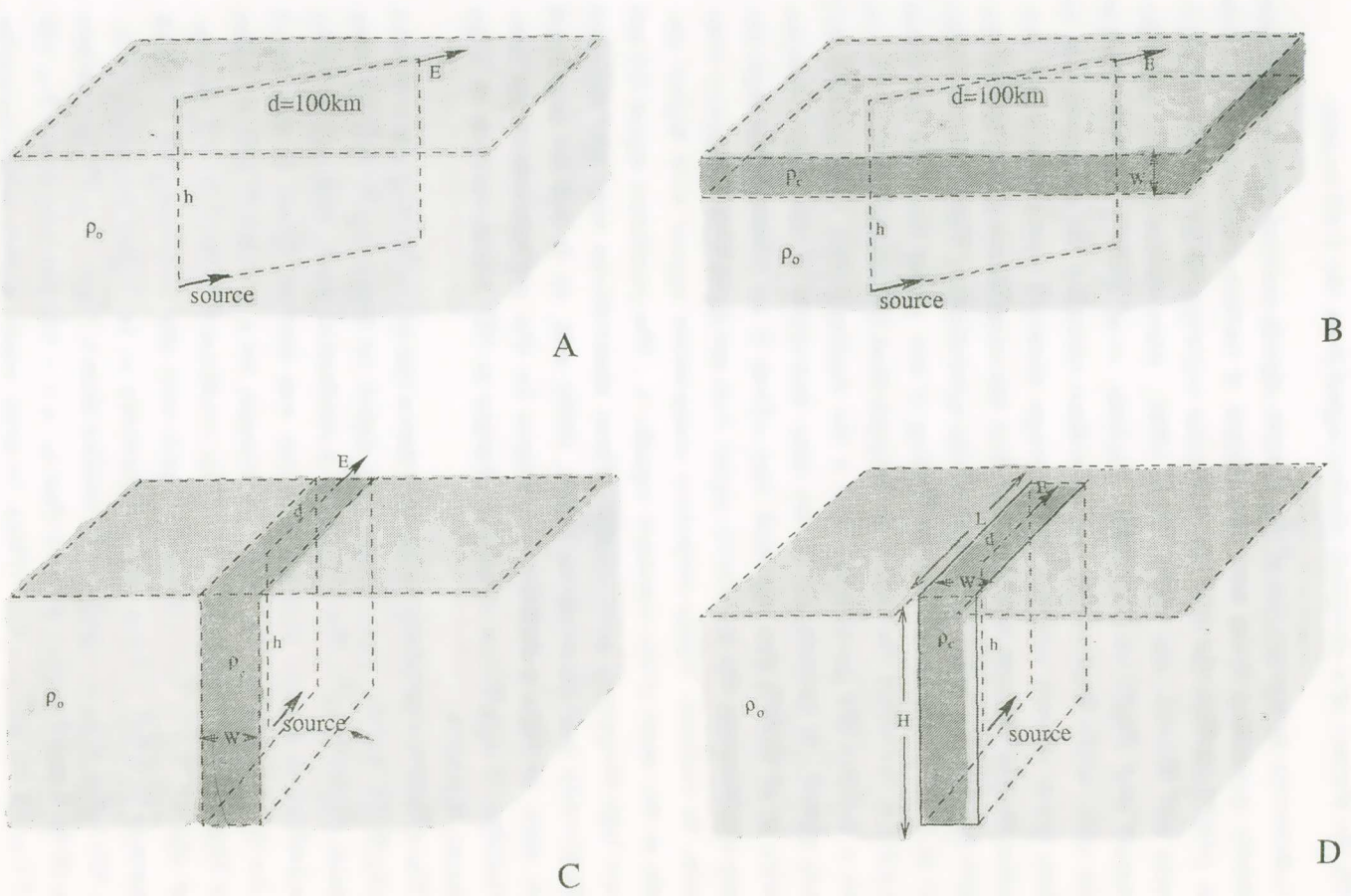

Fig. 5. Schematic representation of the models treated up to date by other authors.

strongly attenuated at distances of the order of 100 km (and hence they cannot be observed), while the SES, i.e., the preseismic signals with $f \leq 0.1$ Hz, can be detected.

b. Additional comments on the Explanation of the SES selectivity effect

VAN group reported (*Varotsos and Lazaridou* [1991]; *Varotsos et al.* [1993]) the so called *selectivity effect*, i.e., SES are observed only at particular

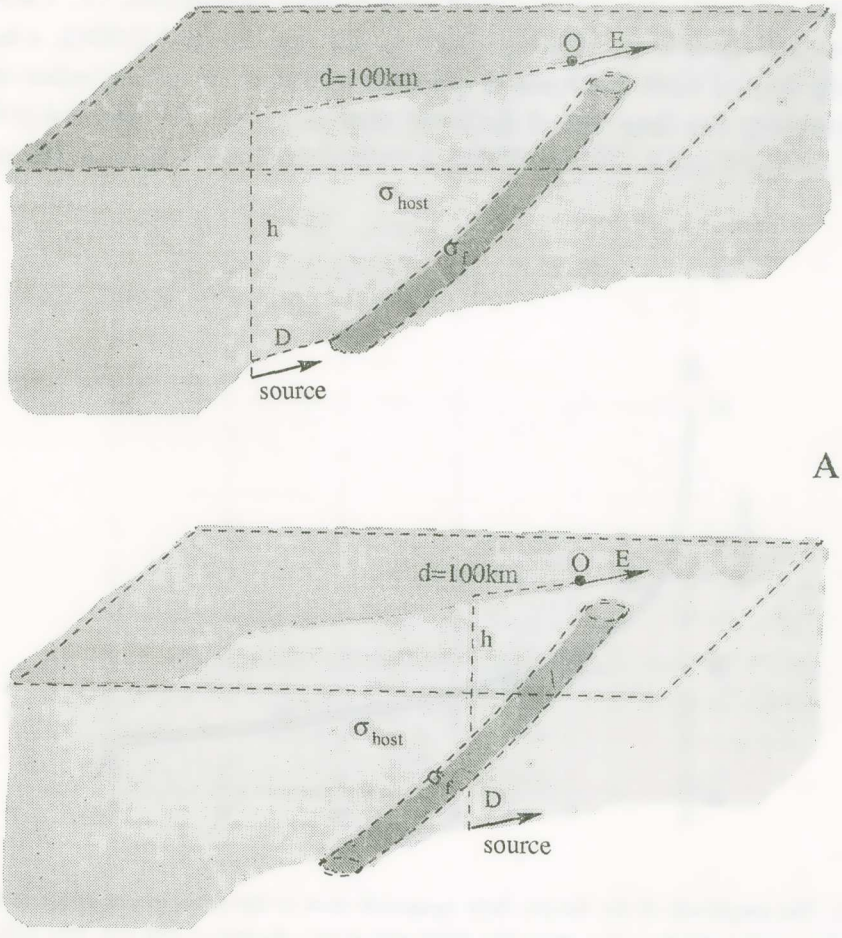

Fig. 6. Schematic representation of the model suggested by Varotsos and coworkers for the explanation of the *selectivity effect*. The case B might be closer to the real situation.

sites of the earth's surface («sensitive sites»), that may lie at long epicentral distances (e.g., $\sim$ 100 km).

Several calculations (*Bernard* [1991; 1992; 1997]; *Bernard and Le Mouel* [1996]; *Park et al.* [1996]; *Neal and Park* [1997]) question the possibility that a reasonable current source (at the earthquake preparation area) can lead to detectable SES at epicentral distances (d) of the order of d $\sim$100 km and suggest (*Bernard* [1992]; *Park et al.* [1996]; *Neal and Park* [1997]) as an alternative possibility, that the source lies close to the measuring (sensitive) site. Figure 5 depicts schematically various models used in these calculations, i.e., a homogeneous half-space (e.g., with resistivity ρ_0, Fig. 1A, *Bernard* [1991]), a horizontally-layered earth (with one or more horizontal layers having resistivities ρ_c appreciably less than that of the lower medium ρ_0, Fig. 1B, *Bernard* [1992; 1997]; *Bernard and Le Mouel* [1996]), a vertical conductive layer ρ_c [either of

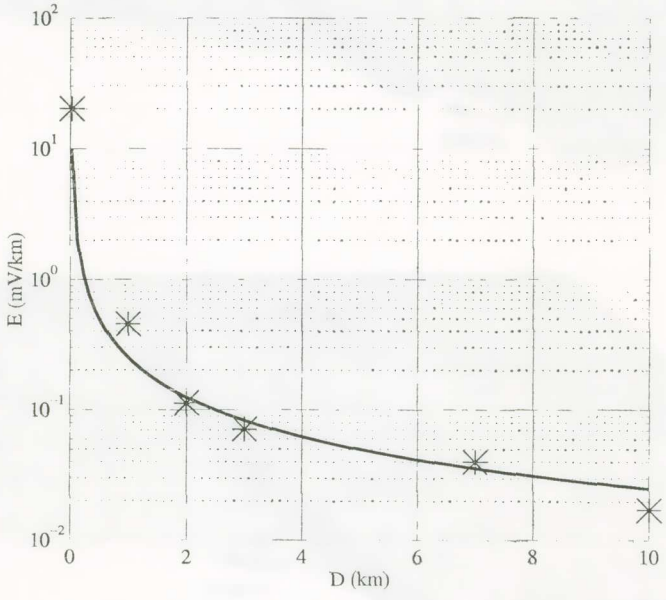

Fig. 7. The amplitude of the electric field measured close to the outcrop versus the distance D of the current dipole source from the other end of the channel in Fig. 6A. The solid line corresponds to 0.25/D and was drawn as a guide to the eye. The values refer to the point (-2 km,0) where (0,0) corresponds to the projection of the outcrop on the earth's surface (see *Varotsos et al.* [1996]). The source was assumed 22.6 A km, i.e., comparable to that taken by Slifkin [1996].

infinite extent, (e.g., see *Park et al.* 1996; or with a length L, *Neal and Park* 1997) appreciably larger than d ~100 km, see Figs 1C, 1D respectively], with a certain width w, embedded in a more resistive half-space ρ_0.

Varotsos and coworkers (*Varotsos and Alexopoulos* [1986]; *Varotsos et al.* [1993]) suggested, long ago, the following model for the SES transmission (Fig. 6): When the SES is emitted, the current dipole source lies in the vicinity of a highly conductive path and hence most of the current is conducted through this path (recall that EQs occur by slip on faults the conductivity σ_f of which is much larger that that of the surrounding medium). Therefore, if the measuring station lies at a site (e.g., see the point «O», on the earth's surface, in Fig. 6) with appreciably higher resistivity than that of the conductive path, but close to the top of this path, the electric field E reaches values which are comparable to those measured by VAN (i.e., 10mV/km, see also Figs 7 and 8). The validity of this model has been recently quantitatively demonstrated, either by numerical solution of Maxwell equations (*Varotsos et al.* [1996;

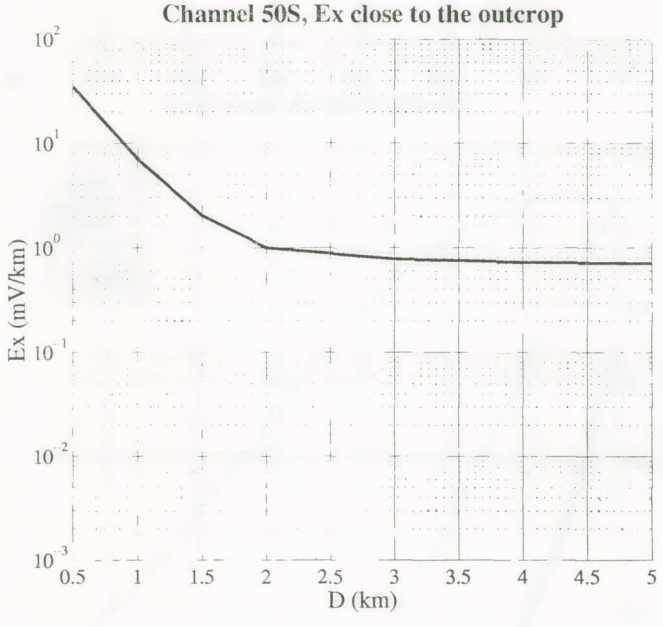

Fig. 8. The amplitude of the electric field measured close to the outcrop versus the distance D of the surrent dipole source from the channel in Fig. 6B. The study corresponds to the values given in Fig. 11 C (i.e., to a sheet with conductance 50 S and a source of 22.6 A km.).

1997b]) —using the EM1DSH (*Hoversten and Becker* [1995]) program (cf. the two cases depicted in Figs 6A and 6B are discussed in our latter two references respectively)— or by analytical solutions (*Varotsos et al.* [1997a], see also Figs 9). All these solutions coincide with the conclusion that there

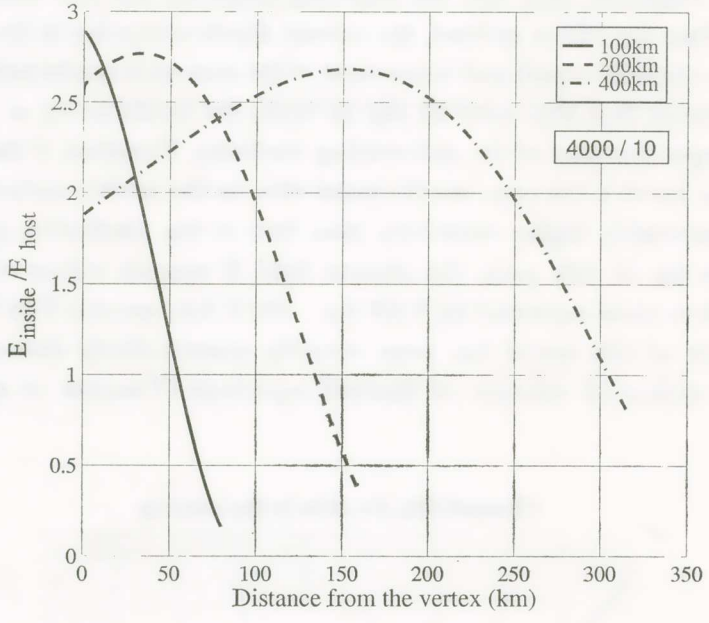

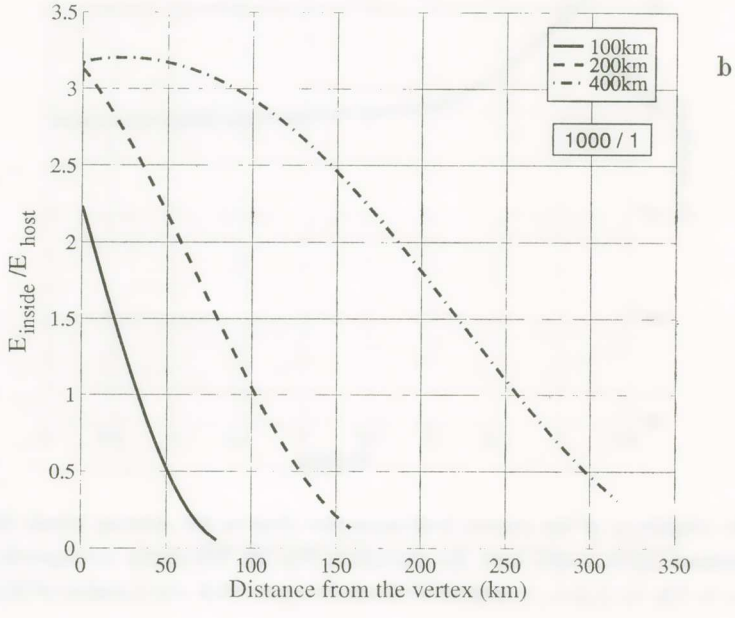

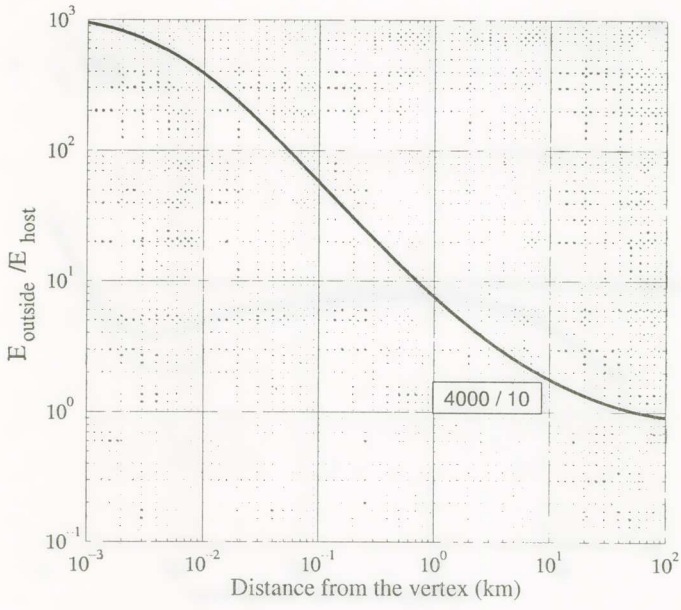
10^3
10^2
10^1
10^0
10^{-1}
$E_{outside}/E_{host}$
4000 / 10
10^{-3}
10^{-2}
10^{-1}
10^0
10^1
10^2
Distance from the vertex (km)

c

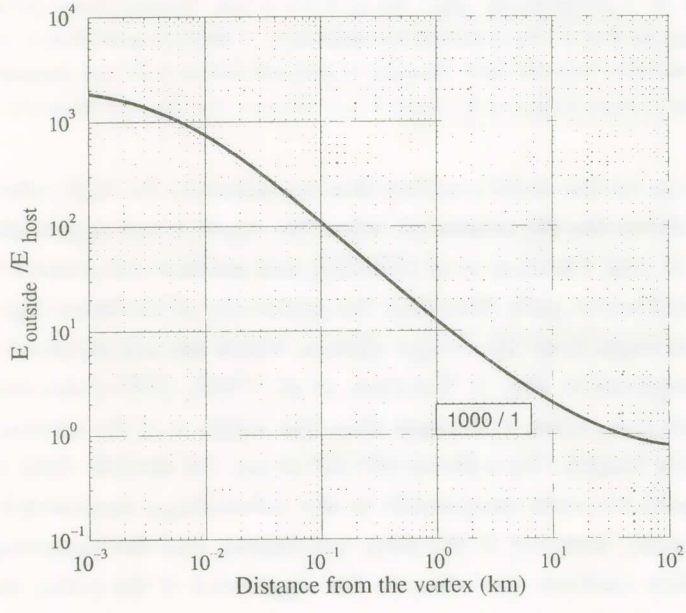
10^4
10^3
10^2
10^1
10^0
10^{-1}
$E_{outside}/E_{host}$
1000 / 1
10^{-3}
10^{-2}
10^{-1}
10^0
10^1
10^2
Distance from the vertex (km)

d

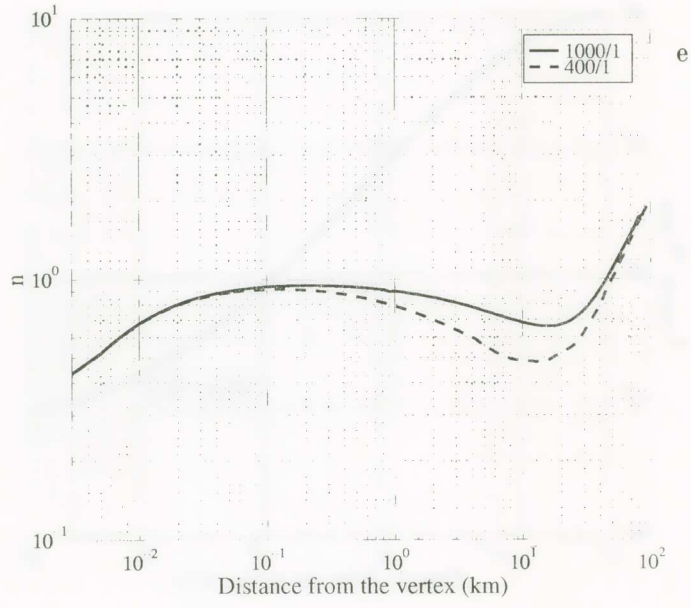

Fig. 9. Study of a paraboloidal edge for $\mu_1 = 0.1\sqrt{km}$. $|E_{inside}|/|E_{host}|$ (a) and (b) and $|E_{outside}|/|E_{inside}|$ (c) and (d) for conductivity ratios $\sigma/\sigma' = 4000/10$ and $1000/1$, respectively. In Fig. (e) we assume that the field $|E_{outside}|$ is proportional to $1/\theta^n$ and determine the exponent n for various distances θ (where θ now denotes the distance from the vertex).

are two regions on the earth's surface that are sensitive for SES collection: one region just above the EQ source (cf. when the depth is not appreciably large, see Figs 10, 11 and *Varotsos et al.* [1997b]), and another one around the upper end of the conductive path. Note that the sensitivity of the latter region almost exclusively emerges from the «*edge effect*», which are not involved in *any* of the models depicted in Fig. 5. *Varotsos et al.* [1996; 1997a] showed that, at long distances (i.e., when d is larger than the width w of the conductive path —with infinite length— by a factor 10^2-10^3 or so), the electric field inside the conductive path becomes comparable to the value (E_{host}) measured if the path were not present; however, if the path terminates, and the measuring site lies in the resistive medium (but close to the upper end of the path), the electric field is enhanced by a factor of the order of σ_f/σ_{host}, and hence it reaches values $\sim E_{host}(\sigma_f/\sigma_{host})$; note that the critical factor of σ_f/σ_{host} —which may be around 10^3— has been disregarded in earlier calculations by other authors.

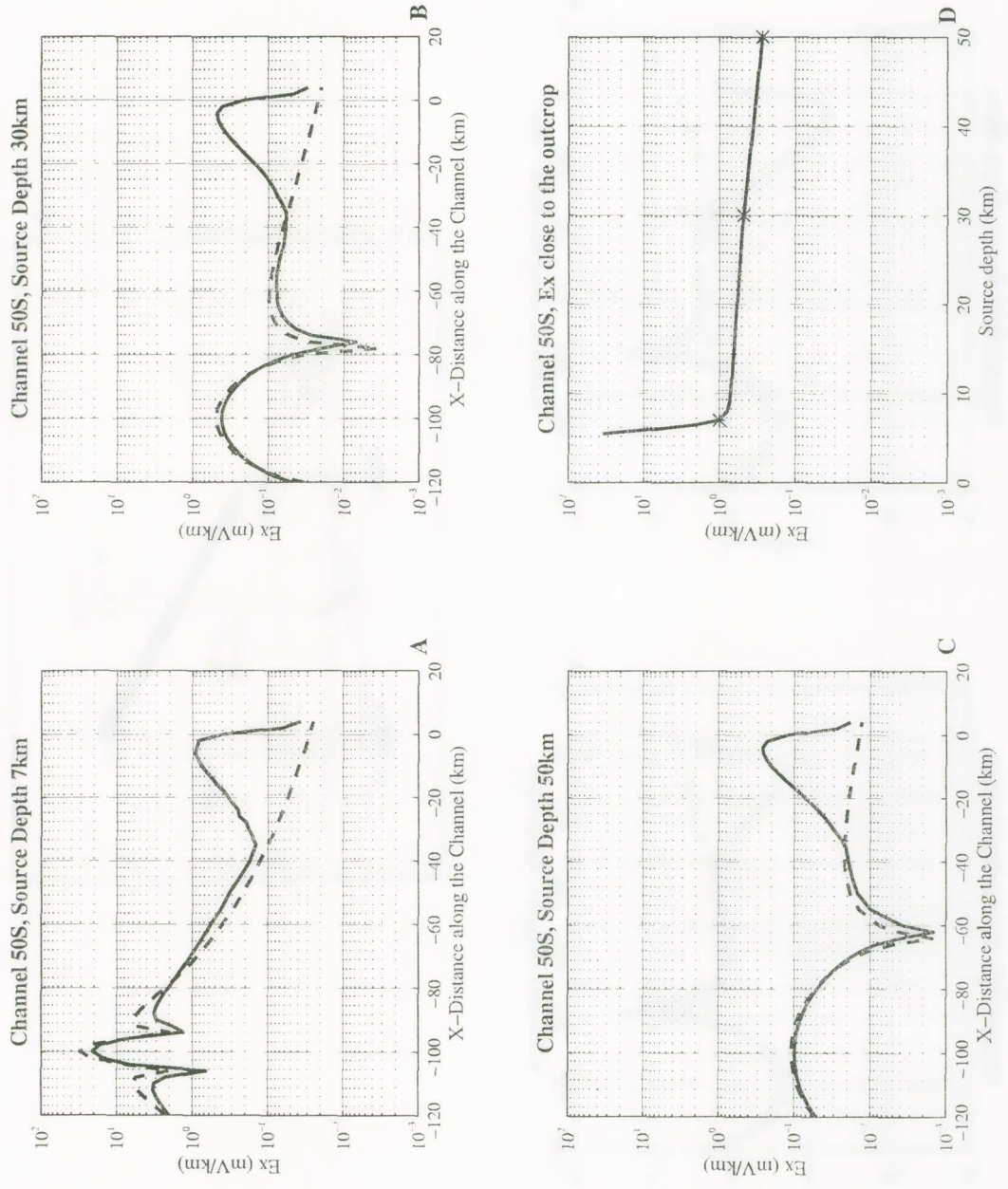

Fig. 10. Variation of the electric field values (Ex)along the channel on the surface of the earth upon increasing the depth of the source. (The source was taken 22.6 Akm). The model is depicted in Fig. 11 C (the broken line corresponds to a two layer earth, i.e., in absence of the channel). Cases A, B and C correspond to depths 7, 30 and 50 km and hence to D = 2, 25 and 45 km.

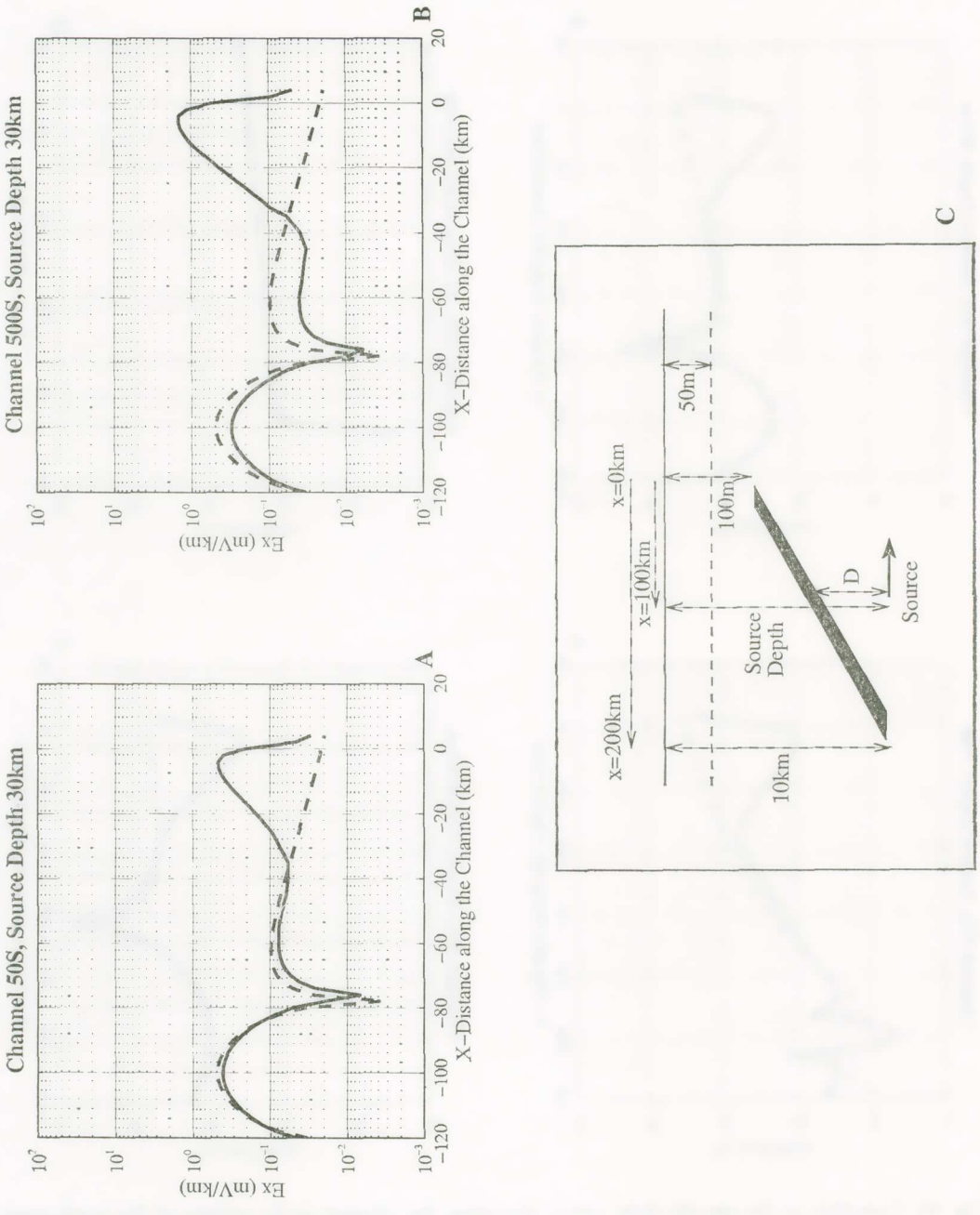

Fig. 11. Variation of the electric field values (Ex) along the channel upon increasing the conductance of the channel (width of 500 m); the source was taken 22.6 A km (the broken line corresponds to a two layer earth, i.e., in absence of the channel).

The following point should be emphasized. The aforementioned explanation of the selectivity effect does not necessarily require a continuous (i.e., non-interrupted) conductive path from the source to the vicinity of the measuring site. What this explanation requires is the existence of a conductive path (cf. in the vicinity of the measuring point, which should lie in the resistive medium but close to the «edge»), the length of which should be appreciably larger (e.g., by a factor 30) than its width (cf. then E_{inside} becomes comparable to E_{host}). In the simple case when the dipole source lies on the principal axis of the path, (and is directed along this axis), although the source may lie at a significant distance from the (closest edge of the) path, e.g. 70 km, the path still acts as a natural amplifier of the electric field, because the measured field (close to the edges) should be of the order of $E_{host}\ \sigma/\sigma'$.

ACKNOWLEDGEMENTS

We would like to express out sincere thanks to Prof. S.Uyeda, Prof.K. Alexopoulos, Prof. G. Dassios for very useful discussions. We also thank Prof. Frank Morrison who drew our attention to the development of EM1DSH program; we also acknowledge with pleasure the continuous help of Dr. M. Hoversten in the application of this programm.

APPENDIX

This can be considered as continuation of the study of the paraboloidal «edge» presented in the Appendix of *Varotsos et al.* [1997a].

We make use of the paraboloidal coordinates

$$x = \lambda\mu\cos(\varphi),\ y = \lambda\mu\sin(\varphi),\ z = 1/2(\lambda^2-\mu^2),$$

and assume that the conductivity in the region $\mu<\mu_1$ bounded by the paraboloidal $\mu = \mu_1$ is σ and for the space outside $\mu\geq\mu_1$ is σ'. We study the case of a point current dipole directed along the z-axis and located at $(0,0,z_0)$. *Varotsos et al.* [1997a] presented, as an example, a calculation for two conductivity ratios, i.e. $\sigma/\sigma' = 4000/10,\ 1000/1$ for the case $\mu_1 = 0.1\sqrt{}(km)$ by considering a dipole source (lying inside the conductive medium) at a distance $z_0 = 100$ km from the vertex of the paraboloid. This calculation showed that close to the vertex $|E_{outside}|/|E_{host}| \approx \sigma/\sigma'$, as expected. It is the scope of this Appendix to draw the attention to the possibility that $|E_{outside}|/|E_{host}|$ may significantly exceed σ/σ'. This can be understood, if we recall the case of the con-

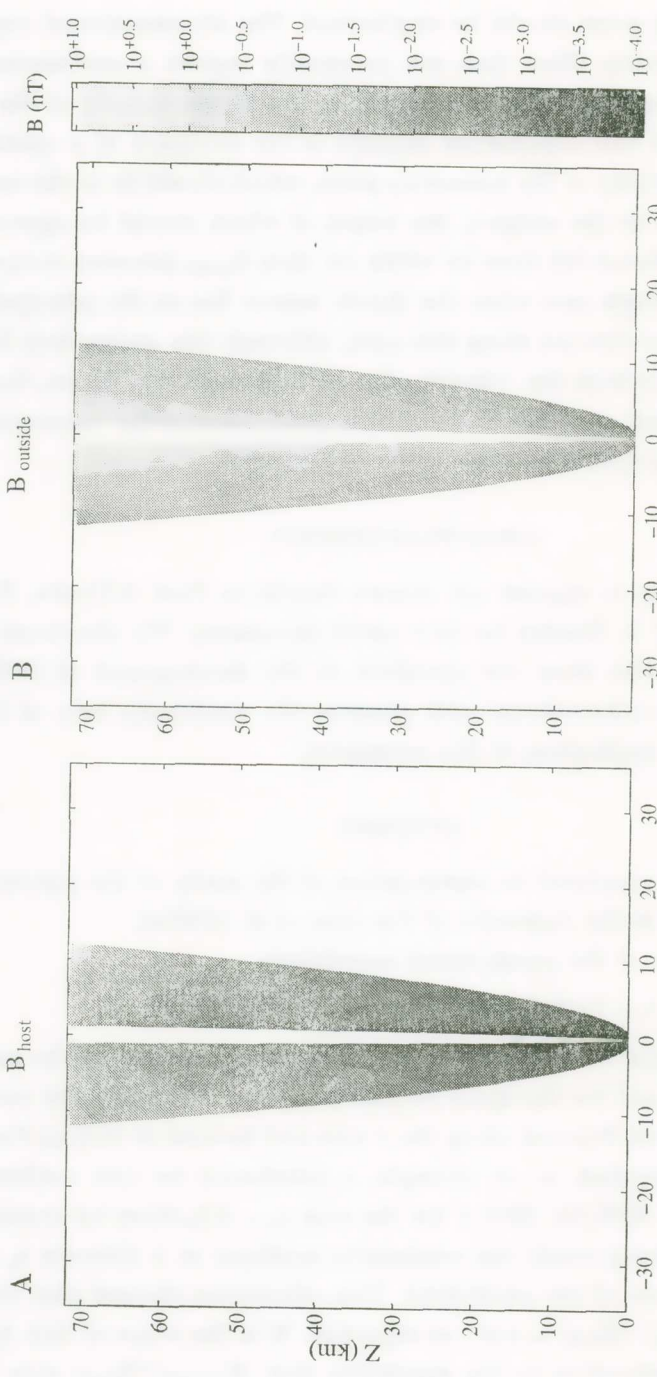

Fig. 12. Study of the magnetic field around a paraboidal edge for $\mu_1 = 0.1\ \sqrt{\text{km}}$ with conductivity ratio $\sigma/\sigma' = 4000/10$. The source was taken 22.6×10^2 A km (*Varotsos et al.* 1997a) located at a distance $z_0 = 100$ km from the vertex. Fig. A corresponds to Bhost, while Fig. B depicts the case when the conductive edge is present.

ductive cylinder, of infinite length; there is a certain region of d/R-values for which $|E_{inside}|/|E_{host}|$ is appreciably larger than unity (see Fig. 2 of *Varotsos et al.* [1997a]); therefore, if the aforementioned distance z_0 of the current dipole from the vertex of the paraboloid belongs to such a region of the d/R-values, we may expect that the ratio $|E_{inside}|/|E_{host}|$ may exceed unity and hence —due to the boundary conditions— $|E_{outside}|/|E_{host}|$ may exceed σ/σ'. Such an example can be seen in Fig. 9. In a and b we plot $|E_{inside}|/|E_{host}|$ for two conductivity ratios, $\sigma/\sigma' = 4000/10$ and $1000/1$ respectively; the calculation was made for various distances $z_0 = 100,200$ and 400 km and confirms that close to the vertex there are some cases (e.g. $z_0 = 100$ and 200 km in Fig. 9a; $z_0 = 200$ and 400 km in Fig. 9b) for which $|E_{inside}|/|E_{host}|$ significantly exceeds unity. In Figs. 9c and 9d we plot $|E_{outside}|/|E_{host}|$ (for the aforementioned two conductivity ratios) and we actually confirm that, in these cases, the ratio $|E_{outside}|/|E_{host}|$ is larger than σ/σ' very close to the vertex. If δ denotes the distance, along $\hat{\mathbf{e}}_\mu$, from the surface of the paraboloid, we find $E_{outside} \propto 1/\delta$ (for distances of the order 10^2 to 10^4m), thus leading to $\Delta V/L \approx$ const when comparing the corresponding values of a long dipole and a short dipole (directed along $\hat{\mathbf{e}}_\mu$).

We now turn to magnetic field (B) calculations. Fig. 12B shows the values of $B_{outside}$ calculated for the paraboloidad edge discussed in Fig. 9, while Fig. 12A depicts the field B_{host}, i.e., in absence of the conductive inset. The calculations were intentionally made for a current dipole $Il = 22.6 \times 10^2$ A km which might correspond to a M 5.0 EQ (*Varotsos et al.* 1997a). Recall that for an x-directed dipole $Il = 1A \times 1$ km (at a depth of 5 km), Fig. 5b of Varotsos et al. (1996) (see the curves labelled «1.0 and 3.0 km layered») indicates that for a layered earth B_y $(= B_{host}) = 10^{-5}$nT at a distance 100 km or so; this reflects a value of the order of $B_y \simeq 10^{-2}$nT for the present source of 22.6×10^2 A km. By comparing this result with Fig. 12B, we find that there are points in a region surrounding the edge (cf. with a «width» $\lambda\mu$ of the order of 1 km of a distance =10 km from the vertex) in which $B_{outside}$ lies in the range of $10^{-2} - 10^{-1}$nT. (i.e., larger than in the case of the layered earth). However, such values are not measurable, and hence we should consider an appreciably stronger source (i.e., a larger magnitude EQ) in order to find detectable B-variations (simultaneously with SES at the «sensitive sites»). This conclusion is the same with that deduced from the numerical B-calculations of Varotsos et al. (1996), but the scattered field values of the latter seem to be significantly overestimated when compared to the present analytical results.

ΠΕΡΙΛΗΨΗ

Ένα πιθανὸ πρότυπο γιὰ τὴν ἐξήγηση τῆς ἐπιλεκτικότητας τῶν Σεισμικῶν Ἠλεκτρικῶν Σημάτων (SES). ΙΙ.

Ἡ παροῦσα ἐργασία εἶναι συνέχεια ἐκείνης ποὺ ἐδημοσιεύθη στὰ Πρακτικὰ τῆς Ἀκαδημίας Ἀθηνῶν, **71** (Α' τεῦχος), 283-354, 1996. Ἡ ἐργασία αὐτὴ μελετᾶ τὴν μεταβολή, συναρτήσει τῆς συχνότητας, τοῦ ἠλεκτρικοῦ πεδίου ποὺ δημιουργεῖ ἕνα δίπολο ρεύματος, ὅταν εὑρίσκεται μέσα (ἢ πολὺ κοντὰ) σὲ πολὺ ἀγώγιμο κύλινδρο ἀπείρου μήκους, ἐμβαπτισμένο σὲ ὑλικὸ πολὺ μεγαλύτερης εἰδικῆς ἀντίστασης. Ἡ μελέτη ἐπεκτείνεται καὶ στὴν περίπτωση ποὺ τὸ δίπολο ρεύματος εἶναι βυθισμένο μέσα σὲ (ἢ πολὺ κοντὰ) σὲ πολὺ ἀγώγιμο στρῶμα ἐβαπτισμένο σὲ ὑλικὸ μὲ πολὺ μεγαλύτερη εἰδικὴ ἀντίσταση. Ἀποδεικνύεται τελικὰ ὅτι, γιὰ συχνότητες μικρότερες ἀπὸ 0.1 Hz, τὸ δημιουργούμενο ἠλεκτρικὸ πεδίο ἔχει ἀνιχνεύσιμες τιμὲς σὲ ἀποστάσεις τῆς τάξεως τῶν 100 km. Ἔτσι ἐξηγεῖται ὅτι τὰ Σεισμικὰ Ἠλεκτρικὰ Σήματα (SES) δίδουν ἀνιχνεύσιμες τιμὲς σὲ ἐπικεντρικὲς ἀποστάσεις τῆς τάξεως τῶν 100 km, ἐνῶ τὰ ἠλεκτρικὰ σήματα ποὺ παράγονται ταυτόχρονα μὲ τὴν θραύση (δηλ. μὲ τὴν γένεση τῶν σεισμῶν) ἀποσβέννυνται, ἐπειδὴ εἶναι σήματα πολὺ μεγαλυτέρας συχνότητας (f>>0.1 Hz). Ἐπίσης ἐξηγεῖται ὅτι τὰ φαινόμενα «ἀκμῆς» (edge effects) διαδραματίζουν πρωτεύοντα ρόλο γιὰ τὴν ἐξήγηση τῆς «ἐπιλεκτικότητας» τῶν Σεισμικῶν Ἠλεκτρικῶν Σημάτων.

REFERENCES

Abramowitz M. and I. Stegun, *Handbook of Mathematical Functions*, Dover, New York, 1970.

Bernard P., Electrical and Seismic Precursors: Theoretical Plausibility of Long Distance Observations, *Eos Trans. AGU, 72*, 44, 329, 1991.

Bernard P., Plausibility of long distance electrotelluric precursors to earthquakes, *J. Geophys. Res., 97*, 17531-17546, 1992.

Bernard P. and Le Mouel J. L., in *The Critical Review of VAN: Earthquake Prediction from Seismic Electric Signals*, ed. Sir J. Lighthill, World Scientific Publishing Co., Singapore, 118-152, 1996.

Bernard P., *Geoph. J. Int.*, 1997 (in press).

Goubeau G., Surface waves and their application to transmission lines, *J. Appl. Phys.* 21, 1119-1128, 1950.

Gradshteyn I. S. and I. M. Ryzhik, *Table of Integrals, Series and Products*, Academic Press, San Diego, 1980.

Hadjicontis V. and C. Mavromatou, Transient electric signals prior to rock failure under uniaxial compression, *Geophys. Res. Lett.*, 21, 1687-1690, 1994.

Hadjicontis V. and C. Mavromatou, Electric signals recorded during uniaxial compression of rock samples: their possible correlation with preseismic electric signals, *Acta Geophys. Pol. XLIII, 1,* 49-61. 1995.

Hadjicontis V. and C. Mavromatou, Laboratory investigation of the electric signals preceding earthquakes, in *The Critical Review of VAN: Earthquake Prediction from Seismic Electric Signals*, ed. Sir J. Lighthill, World Scientific Publishing Co., Singapore, pp. 105-117, 1996.

Hoversten G. M. and A. Becker, EM1DSH with EMMODEL a MotifGUI, Numerical Modelling of multiple thin 3D sheets in a layered earth, University of California at Berkeley, Engineering Geoscience Department (June 12, 1995).

Mavromatou C. and V. Hadjicontis, Laboratory investigation of transient electric signals detected by the VAN network in Greece, in *Electromagnetic Phenomena Related to Eartquake Prediction*, edited by M. Hayakawa and Y. Fujinawa, pp. 293-305, TerraPub, Tokyo, 1994.

Mavromatou C., Laboratory study of electric signals emitted before the fracture of crystalline solids, Ph. D. Thesis, University of Athens, Athens 1995.

Morse P. M. and H. Feshbach, *Methods of Theoretical Physics*, Mc Graw-Hill, New York, 1953.

Neal S. L. and Park S. K. in *Abstract Volume, IASPEI 1997 Conference*, p. 308, Thessaloniki 1997.

Park S. K., Strauss D. J. and Aceves R. L., in *The Critical Review of VAN: Earthquake Prediction from Seismic Electric Signals*, ed. Sir J. Lighthill, World Scientific Publishing Co., Singapore, pp. 267-285, 1996.

Schelkunoff S. A., Transmission Theory of Plane Electromagnetic Waves, *Proc. Intl. Radio Engrs*, 25, 1457-1492, November, 1937.

Schelkunoff S. A., *Electromagnetic Waves*, D. Van Nostrand, Netherlands, 1943.

Slifkin L., A dislocation model for seismic electric signals, in *the Critical Review of VAN: Earthquake Prediction from Seiesmic Electric Signals*, ed., Sir J. Lighthill, World Scientific, Singapore, 97-104, 1996.

Sommerfeld A., «*Electrodynamics*» in Lectures on Theoretical Physics, pp. 178-190, Academic Press, New York, Fourth Printing, 1967.

Stratton J. A., *Electromagnetic Theory*, p. 350, Mc Graw-Hill, New York, 1941.

Uyeda S., Introduction to the VAN method of earthquake prediction, in *The Critical Review of VAN: Earthquake Prediction from Seismic Electric Signals*, ed. Sir J. Lighthill, World Scientific Publishing Co., Singapore, 3-28, 1996.

Varotsos P. and Alexopoulos K., Stimulated current emission in the earth and related geophysical aspects, in *Thermodynamics of Point Defects and their Relation with Bulk Properties*, edited by S. Amelinckx, R, Gevers and J. Nihoul, pp. 136-142, 403-406, 410-412, 417-420, North Holland, Amsterdam, 1986.

Varotsos P. and M. Lazaridou, Latest aspects of earthquake prediction in Greece based on Seismic Electric Signals, *Tectonophysics*, 188, 321-347, 1991.

Varotsos P., K. Alexopoulos and M. Lazaridou, Latest aspects of earthquake prediction in Greece based on Seismic Electric Signals, II, *Tectonophysics*, 224, 1-37, 1993.

Varotsos P., N. Sarlis, M. Lazaridou and P. Kapiris, A plausible model for the explanation of the selectivity effect of Seismic Electric Signals, *Practika of Athens Academy*, 71, 283-354, 1996.

Varotsos P., N. Sarlis, M. Lazaridou and P. Kapiris, Transmission of stress induced electric signals in dielectric media, *J. Appl. Phys.* 1997a, (to be published).

Varotsos P., N. Sarlis, M. Lazaridou and P. Kapiris, A possible explanation for detecting Seismic Electric Signals at certain sites of the earth's surface, *Earth Observation and Remote Sensing* 1997b, (in press).

Ward S. H. and G. W. Hohmann, in *Electromagnetic Methods in Applied Geophysics, Volume 1, Theory*, Edited by Nambighian, M. N. pp. 203-252, Society of Exploration Geophysicists, Tulsa Oklahoma, 1994.

Yoshida S., M. Uyeshima and M. Nakatani, Electric potential changes associated with slip failure of granite: Preseismic and coseismic signals, *J. Geophys. Res.*, 102, 14883-14897, 1997.